The influence of key residues in the tunnel entrance and the active site on activity and selectivity of toluene-4-monooxygenase

Moran Brouk, Netta-Lee Derry, Janna Shainsky, Zohar Ben-Barak Zelas, Yulia Boyko, Keren Dabush, Ayelet Fishman *

Department of Biotechnology and Food Engineering, and Institute of Catalysis Science and Technology, Technion-Israel Institute of Technology, Haifa 32000, Israel

ARTICLE INFO

ABSTRACT

Site-directed saturation mutagenesis is a convenient method to fine tune enzyme activity and selectivity at known "hot spots". The objective of this work was to investigate the influence of mutations in the tunnel entrance of toluene 4-monooxygenase (T4MO) from *Pseudomonas mendocina* KR1 on rate, regioselectivity, and enantio-selectivity, in comparison with mutations located in the active site. Residue TmoA D285, located at the tunnel entrance, distant from the active site was randomized, as well as residue I100 which is positioned in the vicinity of the diiron center. Both libraries were screened for regioselective hydroxylation of phenylethanol (PEA), and enantioselective oxidation of methyl *p*-tolyl sulfide and styrene. It was discovered that mutations at position 285 enhanced the rate of catalysis but did not affect the specificity. Substitutions D285I and D285Q were beneficial for the oxidation of the large and bulky substrates PEA and methyl *p*-tolyl sulfide (8–11-fold improvement), however variant D285S improved the activity rate for styrene oxidation (1.7-fold). Thus, the extent of improvement in rate, and the best amino acid replacement were substrate dependant. In contrast, mutations at position I100 influenced the activity rate and the selectivity for all three substrates tested. Combining the effects by mutating both "gates", to the tunnel entrance along with the active site, resulted in an additive or even synergistic outcome on enzyme activity and selectivity.

© 2010 Elsevier B.V. All rights reserved.

1. Introduction

Naturally occurring enzymes are remarkable biocatalysts with numerous potential applications in organic synthesis, industry and medicine. One of the main advantages of biocatalysts, in addition to their high regio- and enantio-selectivity, is their ability to accept substrates other than their natural ones [1,2]. However, enzyme activity on non-natural compounds is often much lower than on the natural substrate. Several protein engineering techniques have been developed in order to overcome the limitations of natural enzymes and to design enzymes for specific applications. These techniques can be roughly divided into two main strategies: rational design and directed evolution [3].

Rational design uses detailed knowledge about the enzyme structure and function in order to identify precise residue(s) which can be mutated for designing or improving a specific quality of the enzyme [4,5]. In contrast to the comprehensive understanding required for rational design, directed evolution is based on the Darwinian principles of mutation and selection and does not require prior knowledge regarding the structure [2,3]. In directed evolution, random mutations are generated on the gene of interest thus creating a diverse library, which is screened for the desirable quality.

In between these two strategies lies site-specific saturation mutagenesis that can be used to introduce all possible amino acids at any predetermined position in a gene. This semi-rational approach can provide more comprehensive information than can be gained by a single amino acid substitution, as well as overcome the drawbacks and biases of random mutagenesis (e.g. incompleteness of the amino acid diversity introduced and the need for high-throughput screening) [6,7]. Site-specific saturation mutagenesis enables the fine-tuning of enzyme structure by "finding" the best amino acid at a specific position.

Often, when changes in the catalytic properties of an enzyme are sought (such as regio- and enantio-selectivity, substrate specificity and alternative catalytic activity) mutations close to the active site appear to be more effective than distant ones. For improving protein activity and stability (such as thermostability or stability toward organic solvents), both close and distant mutations have been shown to be useful [5,8].

Relatively few studies have investigated the effect of mutating residues located in the tunnel or tunnel entrance, leading to the active site. Vardar et al. found that mutating a residue located in the entrance of the tunnel in toluene-*ortho*-xylene monooxygenase

* Corresponding author. Tel.: +972 4 829 5898; fax: +972 4 829 3399.
  E-mail address: afishman@tx.technion.ac.il (A. Fishman).

of *Pseudomonas stutzeri* OX1, influences the catalysis rate of the enzyme, whereas the regiospecificity remained the same [9,10]. Furthermore, it was shown by Schmitt et al. that modifications made in the tunnel of *Candida rugosa* lipase can alter the activity of the enzyme towards fatty acids with different chain lengths (the activity was decreased when the chain was long enough to reach the mutated site) [11]. Capila et al. used site-specific mutagenesis to change a residue within the active site tunnel of chondroitin AC lyase which affects the binding affinity and causes a change in the action pattern of the enzyme [12]. Chaloupková et al. reported that the effect of mutating a residue located at the tunnel entrance of haloalkane dehalogenase from *Sphingomonas paucimobilis* UT26, on the enzyme activity varied with the structure of the substrate, but in general, the activity increased with the introduction of small and nonpolar amino acids [13]. Recently, Pavlova et al. investigated key residues in access tunnels of *Rhodococcus rhodochrous* haloalkane dehalogenase and described the influence of these residues on the substrate and water passage to the active site [14].

In the present study, site-specific saturation mutagenesis was used to investigate a key residue in the tunnel entrance of toluene-4-monooxygenase (T4MO) from *Pseudomonas mendocina* KR1. T4MO, belonging to the toluene monoxygenase (TMO) family, is a soluble four-component enzyme which hydroxylates toluene primarily at the *para* position forming 96% *p*-cresol. Other extensively studied TMOs are toluene *ortho*-monooxygenase (TOM) of *Burkholderia cepacia* G4 [15], toluene *ortho*-xylene monooxygenase (ToMO) of *Pseudomonas stutzeri* OX1 [10,16] and toluene *para*-monooxygenase (TpMO) of *Ralstonia pickettii* PKO1 [6,17]. T4MO consists of a 211-kDa hydroxylase which contains the catalytically active diiron center and is composed of two subunits in an $(\alpha\beta\gamma)_2$ quaternary structure [18,19]. The other components are a 36-kDa NADH oxidoreductase, a 12.5-kDa Rieske-type [2Fe–2S] ferredoxin, and a 11.6-kDa effector protein [19–21].

It was our objective to investigate the influence of mutations in the tunnel on rate, regioselectivity, and enantio-selectivity of T4MO, in comparison with mutations located in the active site. Various substrates were investigated to study the generality of tunnel entrance mutagenesis in T4MO.

2. Materials and methods

2.1. Chemicals

2-Phenylethanol (PEA), *o*-, *m*-, *p*-tyrosol, methyl-*p*-tolyl sulfide, (R)- and (S)-methyl-*p*-tolyl sulfoxide and N,O-Bis(trimethylsilyl)-acetamide were purchased from Sigma–Aldrich Chemical Co. (Sigma–Aldrich, Rehovot, Israel). Toluene was purchased from Bio-Lab (Jerusalem, Israel). Hydroxytyrosol was obtained from Cayman Chemical Co. (MI, USA). Styrene, styrene oxide, (R)-styrene oxide and *p*-nitrothiophenolate were purchased from Acros Organics (Holland Moran, Yahud, Israel). All standards were prepared as stock solutions in ethanol. All materials used were of the highest purity available and were used without further purification.

2.2. Bacterial strains and growth conditions

Escherichia coli TG1 (*supE hsd*Δ5 *thi* Δ(*lac-proAB*) F' [*traD*36 *proAB*+ *lacI*q *lacZ*ΔM15]) with the plasmid constructs was routinely cultivated at 37 °C in Luria-Bertani (LB) medium [22] supplemented with kanamycin at 100 μg/ml to maintain the plasmids. To stably and constitutively express the toluene monooxygenase genes from the same promoter, the expression vectors pBS(Kan)TOM (henceforth TOM) [15] pBS(Kan)TpMO (henceforth TpMO) [23], pBS(Kan)ToMO (henceforth ToMO) [24] and pBS(Kan)T4MO (henceforth T4MO) [23], were constructed as

described earlier. All experiments were conducted as described previously [25,26]. Concisely, overnight cells were diluted to an optical density (OD) at 600 nm of 0.1 and grown to an OD of 1.3. The exponentially grown cells were centrifuged (8000 × *g* for 10 min at 25 °C) and re-suspended in potassium phosphate buffer (100 mM, pH 7.0). Cells were subsequently used in biotransformation protocols as described later on. Expression of TMOs (wild-type [WT] and variants) by pBS(Kan) vectors within *E. coli* strains produced blue or brown cells on agar plates and in broth cultures. The color is indicative of indigoid compounds formed by oxidation of indole from tryptophan [27,28].

2.3. Protein analysis and molecular techniques

Protein samples of cells grown with and without 1 mM isopropyl β-D-thiogalactopyranoside (IPTG) were analyzed on standard 12% Lammeli discontinuous sodium dodecyl sulfate (SDS)-polyacrylamide gels [22]. All of the highly active enzyme variants were analyzed by SDS-PAGE to ascertain that the increase in activity is the result of the desired mutation rather than unexpected changes in expression level.

Plasmid DNA was isolated using a Mini Kit (Qiagen, CA, USA), and DNA fragments were collected using the E-gel® CloneWell™ system comprised of 0.8% SYBR Safe™ gels, and E-gel® iBase™ as the electrophoresis unit (Invitrogen, Carlsbad, CA). Transformation of plasmids into *E. coli* cells was performed via electroporation using a Micro-Pulser instrument (Bio-Rad, CA, USA) with the program Ec1 (1.8 kV, 1 pulse for a 0.1 cm cuvette).

2.4. Site-specific saturation mutagenesis

A gene library encoding all possible amino acids at position TmoA D285 in T4MO was constructed as described previously [26]. To randomize position 285, two degenerate primers, T4MO_285_Front and T4MO_285_Rear (Table 1), were designed as well as primers T4MObefEcoRI Front (upstream of the unique EcoRI site and the start codon of *tmoA*) and T4MOABRear (downstream of the stop codon of *tmoB* and the unique AatII site). The first degenerate PCR fragment was amplified using primers T4MO_285_Front and T4MOABRear, while the second was amplified using primers T4MObefEcoRI Front and T4MO_285_Rear. The PCR program consisted of an initial denaturation at 94 °C for 2 min, followed by 25 cycles of 94 °C for 45 s, 55 °C for 45 s, and 72 °C for 2.2 min, with a final extension at 72 °C for 8 min. The two fragments were combined during the final reassembly PCR in a 1:1 molar ratio using the

Table 1
Primers used for saturation mutagenesis, site-directed mutagenesis and sequencing of the D285 region in the *tmoA* gene in TG1/pBS(Kan)T4MO.

Primer	Nucleotide sequence[a]
Mutagenesis	
T4MObefEcoRI Front	5′-CCATGATTACGCCAAGCGCG-3′
T4MOABRear	5′-TCCATGCTCTTCACTGTTGAC-3′
T4MO_285_Front	5′-GGATTACTACACGCCGTTGGAG**NNN**CGCAGCCAG-3′
T4MO_285_Rear	5′-AACTCCTTGAATGACTGGCTGCG**NNN**CTCCAACGG-3′
T4MO_285Q_Front	5′-GGATTACTACACGCCGTTGGAG**CAG**CGCAGCCAG-3′
T4MO_285Q_Rear	5′-AACTCCTTGAATGACTGGCTGCG**CTG**CTCCAACGG-3′
T4MO_285I_Front	5′-GGATTACTACACGCCGTTGGAG**ATC**CGCAGCCAG-3′
T4MO_285I_Rear	5′-AACTCCTTGAATGACTGGCTGCG**GAT**CTCCAACGG-3′
T4MO_100L_Front	5′-CACTTTGAAATCCCATTACGGCGCC**CTC**GCAGTTGG-3′
T4MO_100L_Rear	5′-GCTGCATATTCACCAACTGC**GAG**GGCGCCGTAATGG-3′
Sequencing	
T4MO seq 1	5′-CCCGCATGAATACTGTAAGAAGGATCGC-3′

N stands for A, T, G or C.

[a] Positions subjected to mutagenesis are underlined and bases modified to obtain the desired point mutation are indicated in bold.

outer primers T4MObefEcoRI Front and T4MOABRear. The assembling PCR was programmed similarly to the above PCR program, with extension at 72 °C for 3.15 min instead of 2.2 min. The assembled PCR fragment, containing randomized nucleotides at position TmoA 285, was ligated into T4MO, after the double digestion of both vector and insert with EcoRI and AatII, replacing the corresponding fragment in the original plasmid. The resulting plasmid library was electroporated into *E. coli* TG1 cells.

The generation of libraries T4MO TmoA I100 and TOM TomA3 V106 was described previously [25,26].

2.5. Site-directed mutagenesis

Site-directed mutagenesis at the T4MO *tmoA* gene was performed via overlap extension PCR, in a similar way to the site-specific saturation mutagenesis. Shortly, three oligonucleotide primer pairs were designed (Table 1) to generate the desired mutations. For generating the D285Q, D285I and I100L mutations, the first mutated PCR fragment was amplified using primers T4MO_285Q_Front, T4MO_285I_Front and T4MO_100L_Front, respectively, together with T4MOABRear. The second mutated PCR fragment was amplified using T4MObefEcoRI primer together with T4MO_285Q_Rear, T4MO_285I_Rear and T4MO_100L_Rear, respectively. In contrast with the saturation mutagenesis protocol, here, T4MO plasmids containing a site mutation (T4MO TmoA I100A, I100G or D285S) were used as templates to create the double mutants I100A/D285Q or D285I, I100G/D285I and I100L/D285S, respectively. Each pair of fragments was combined during the final reassembly PCR using the outer primers T4MObefEcoRI Front and T4MOABRear. The assembled PCR fragment was ligated into WT T4MO, after the double digestion of both vector and insert with EcoRI and AatII, replacing the corresponding fragment in the original plasmid.

2.6. Whole-cell enzymatic biotransformations

Whole-cell activity assays were performed as described previously [25,26]. When using PEA as a substrate, the biotransformation was carried out in screw-capped 16-ml glass vials containing 2 ml cells and 0.25 mM substrate (added from a 100 mM stock solution in ethanol). Twenty-one-millilitre glass vials containing the cell suspensions (2 ml) were used for styrene and methyl-*p*-tolyl sulfide oxidation, due to their volatility. Each vial was sealed with a Teflon-coated septum and aluminum crimp seal, and 1 mM substrates were added by injection with a syringe (added from a 400 mM and 200 mM stock solutions in ethanol, respectively). All the vials were shaken at 600 rpm (Vibramax 100, Heidolph, Nurenberg, Germany) at 30 °C.

The reaction was stopped periodically (a vial was sacrificed) by filtration of the cells or by extraction with 2 ml ethyl acetate containing 0.5 mM *tert* butyl benzene (as an internal standard). Filtration was used for reactions measured by HPLC, whereas, extraction was used for samples analyzed by GC. The negative control used in these experiments was TG1/pBS(Kan) (a plasmid without the monooxygenase). The initial transformation rates were determined by sampling at 3–20 min intervals during the first 2–5 h. The specific activity (nmol/min/mg protein) was calculated as the ratio of the initial transformation rate and the total protein content. Total protein content was 0.22 [mg protein/ml/OD$_{600\,nm}$] for TOM and ToMO and 0.24 [mg protein/ml/OD$_{600\,nm}$] for T4MO and TpMO [16,17,29]. Activity data reported in this paper are based on at least two independent results.

Toluene oxidation was determined in a similar way to styrene and methyl-*p*-tolyl sulfide. Two millilitre of the cell suspensions was sealed in a 21-ml vial. 0.89 mM and 3.56 mM toluene was added to the vial, calculated as if all the substrate was in the liquid phase (the actual initial liquid concentration was 0.25 mM and 1 mM, respectively, based on a Henry's Law constant of 0.27 [30]). The vials were shaken at 30 °C and the reaction was stopped in 2–5 min intervals by injecting 2 ml ethyl acetate containing 0.5 mM *tert* butyl benzene as an internal standard. The vials were mixed thoroughly to ensure complete extraction of the toluene, and the organic phase was separated from the aqueous phase by centrifugation. The samples were analyzed by gas chromatography mass spectra (GC/MS).

2.7. Analytical methods

Specific analytical methods were developed for separation of each of the substrates (and respective products) used in this work.

2.7.1. Hydroxylation of PEA
The progress of enzymatic hydroxylation of PEA was measured by reverse-phase HPLC, whereas the regiospecificity, in addition to structure verification, was determined by GC/MS analysis. The detailed analytical methods were the same as we described previously [25].

2.7.2. Oxidation of methyl-p-tolyl sulfide
Conversion of methyl-*p*-tolyl sulfide to (S)- or (R)-methyl-*p*-tolyl sulfoxide was determined by gas chromatography (GC) equipped with a chiral column and flame ionization detector, and the identity of compounds was confirmed by GC/MS. The detailed analytical methods were the same as described previously [26].

2.7.3. Conversion of styrene to styrene oxide
The epoxidation of styrene was determined in a similar way to oxidation of methyl-*p*-tolyl sulfide using the following changes. The conversion was determined with a GC 6890N instrument (Agilent Technologies, Santa Clara, CA), using a 30 m × 0.32 mm × 0.25 μm capillary column packed with γ-cyclodextrin trifluoroacetyl (Chiraldex G-TA; ASTEC, Bellefonte, PA) and flame ionization detector. The temperature was programmed as follows: $T_1 = 60\,°C$; $dT/dt = 20\,°C/min$, $T_2 = 120\,°C$; $dT/dt = 20\,°C/min$, $T_3 = 100\,°C$, 18 min, split ratio 1:3. Under these conditions, the retention times were: 7.40 min for styrene, 9.67 min for *t*-butyl benzene, 13.10 min for (S)-styrene oxide and 13.78 min for (R)-styrene oxide.

The identity of styrene and styrene oxide was also confirmed by GC/MS, equipped with a capillary HP-5 column (30 m × 0.32 mm × 0.25 μm, Agilent Technologies) and the temperature was programmed as follows: $T_1 = 50\,°C$; $dT/dt = 20\,°C/min$, $T_2 = 170\,°C$, 18 min, split ratio 1:10. Under these conditions, the retention times were: 8.07 min for styrene, 12.49 min for *t*-butyl benzene and 13.78 min for styrene oxide.

2.7.4. Hydroxylation of toluene
The hydroxylation of toluene was determined using GC/MS (Agilent Technologies, Santa Clara, CA), equipped with a capillary HP-5 column (30 m × 0.32 mm × 0.25 μm). The temperature was programmed as follows: $T_1 = 50\,°C$, 4 min; $dT/dt = 30\,°C/min$, $T_2 = 280\,°C$; 0.5 min, split ratio 1:10. Under these conditions, the retention times were: 3.7 min for toluene and 6.8 min for *t*-butyl benzene.

2.8. Screening methods

2.8.1. One-point-biotransformation as a screening method for improved hydroxylation, sulfoxidation and epoxidation activities
Screening for mutants with improved activity towards PEA, methyl-*p*-tolyl sulfide and styrene was performed in a similar way to the whole-cell biotransformation with some simplifications: one

colony of each mutant was inoculated to 5 ml LB medium supplemented with kanamycin (100 μg/ml) and grown for 20 h at 37 °C with shaking at 250 rpm. The cells were centrifuged at 6000 × g for 10 min and re-suspended in 1.5 ml PB (0.1 M, pH 7.0). 0.25 mM PEA, 0.5 mM methyl-*p*-tolyl sulfide or 1 mM styrene was added to 1 ml of cell suspension, which was than shaken at 600 rpm, room temperature for 24 h (2 h for styrene). The remaining cell suspension was used to determine the cell density at 600 nm. The reactions were stopped by centrifugation or extraction as described previously. In order to ensure the probability (99%) that all 64 possible outcomes from the single-site random mutagenesis had been sampled, at least 292 colonies were screened [31].

2.8.2. Screening for improved epoxidation activity using *p*-nitrothiophenolate (pNTP) assay

The detection of styrene conversion to styrene oxide was based on color loss of pNTP in the assay. This colorimetric assay is a modification of the method described by Tee et al. [32,33].

The screening of highly active enzymes was preformed in a 96-plate format, using the *epMotion 5070* robotic system. The T4MO D285 library was screened by, initially, picking colonies from glycerol stocks stored in 96-well plates, using a VP 381 library copier (V&P Scientific, Inc., San Diego, CA). The colonies were transferred to 96-deep-well polypropylene plates (ABgene; Thermo Fisher Scientific, Epson, United Kingdom) containing 1.2 ml of LB medium supplemented with 100 μg/ml kanamycin. Cells were grown (18 h, 37 °C) and precipitated by centrifugation (3000 × g, 10 min), followed by resuspension in 0.4 ml of PB (0.1 M, pH 7.0) containing 1 mM styrene. Tenth ml from each well was removed for measuring the cell density at 600 nm. Following 2 h incubation at room temperature with styrene, the cells were centrifuged (3000 × g, 10 min) and 0.15 ml supernatant was transferred to each well of a 96-well polystyrene plate. Ten microlitre of 12% (w/v) methylated β-cyclodextrin (mβ-CD) in isopropanol and 40 μl of freshly prepared 2.5 mM pNTP in 0.25 M NaOH were added to each well. The plate was shaken for 1 h at room temperature and the absorbance was measured (443 nm) using a microplate reader (Optimax Molecular Devices, Sunny Vale, CA, USA).

In order to validate the accuracy and reproducibility of the screening method, the supernatant was also analyzed by GC.

Preliminary results (data not shown) demonstrated that the total decrease in absorption between 1 mM and 0 mM styrene oxide (parallel to 0–100% conversion) was 0.9. Therefore, mutants showing at least 0.3 U ($Abs_{443\,nm}/OD_{600\,nm}$) decline in absorbance compared to wild-type were considered positive in the screen and chosen for further investigation.

3. Results and discussion

3.1. Site-specific saturation mutagenesis at the tunnel entrance of T4MO hydroxylase

The alpha-subunit of the T4MO hydroxylase contains the diiron catalytic center for substrate binding and it was reported to be responsible for the oxidation activity and selectivity [17,18]. Within the alpha-subunit, a tunnel connects the diiron center to the surface of the protein [19]. The tunnel comprises of a narrow entrance with high negative electrostatic charge. At the mouth of the tunnel lies residue Asp 285 located ~26 Å away from the active site (calculated using the Swiss-PDB viewer).

It was hypothesized that the polar and bulky residue of Asp 285 might control the substrate entrance and product efflux to/from the active site (Fig. 1). Hence, engineering the narrow and polar tunnel entrance in T4MO may improve its performance towards non-natural substrates. Given the entrance distance from the
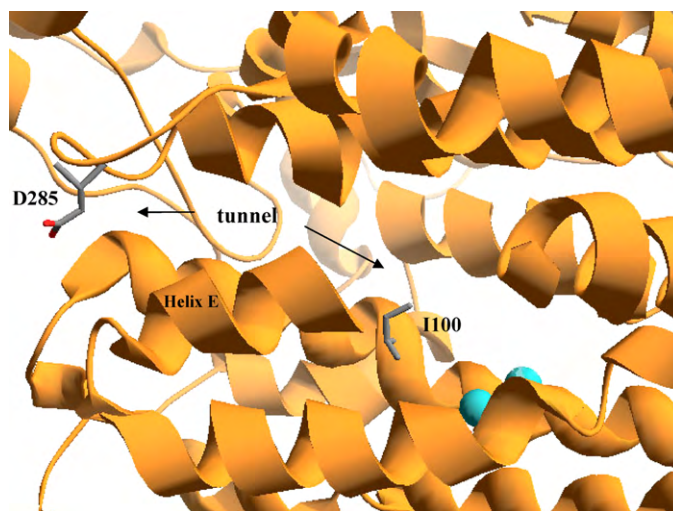
Fig. 1. Positions of key residues in the tunnel entrance (D285) and active site (I100) of the α-subunit of WT T4MO. The tunnel location and key residues, selected for mutagenesis, are indicated in the figure. The Fe atoms are colored as cyan balls. Helix E was truncated between residues 199 and 205 to enable better visualization of the active site. The T4MO hydroxylase was visualized using Swiss-PdbViewer program (PDB code: 3DHG [19]).

catalytic site, it is not expected to influence the catalytic properties of the enzyme such as regio- or enantio-selectivity. For exploring this assumption, site-specific saturation mutagenesis was used to generate a library of T4MO TmoA D285 variants. The variants' activity was screened on three different substrates: hydroxylation of 2-phenylethanol (PEA), oxidation of methyl-*p*-tolyl sulfide and epoxidation of styrene. Since T4MO is a complex multi-component enzyme which requires the recycling of NADH, whole-cells expressing the different T4MO variants were used in all assays.

3.2. The ability of WT T4MO and D285 variants to hydroxylate PEA

PEA (Fig. 2A) is an abundant flavor and fragrance compound with a rose-like odor. Recently, we reported the use of PEA as a starting material for the biosynthesis of hydroxytyrosol, a potent antioxidant found naturally in olives [25].

Out of the four WT TMOs evaluated for their ability to oxidize PEA, WT T4MO had the lowest oxidation rate (Table 2). Comparison between the crystal structures of T4MO [19] and ToMO (exhibiting 68% amino acid identity for the α-subunits) [34], which oxidized PEA 2.2-fold faster, shows a narrower channel entrance in T4MO and with higher negative electrostatic charge. One of the amino acid residues responsible for this difference is located at position 285. This position in ToMO is occupied with Ser which is smaller and less charged than Asp situated in T4MO. Based on pervious results [25], it is assumed that the bulky and hydrophilic nature of the PEA side chain collides with the polar and bulky residue of Asp 285 at the tunnel entrance. Therefore, increasing the width of the entrance may allow higher conversion rates of PEA by T4MO variants.

Consequently, the T4MO TmoA D285 library was screened for increased activity towards PEA. Screening of more than 300 variants was performed to ensure, with a 99% probability, that each of the 64 possible codons is sampled [6]. The 14 variants which oxidized PEA at the highest rate were sequenced to give seven different variants: D285P, D285A, D285Y, D285L, D285C, D285I and D285Q. Unexpectedly, none of them was Ser, the equivalent residue in ToMO.

Table 2
Regiospecific and enantioselective oxidation of PEA, methyl-p-tolyl sulfide and styrene by TG1 cells expressing wild-type TOM, ToMO, T4MO and TpMO.

Substrate	PEA[b]				Methyl-p-tolyl sulfide[c]		Styrene[d]	
Enzyme[a]	Initial oxidation rate (nmol/min/mg protein)	Product distribution			Initial oxidation rate (nmol/min/mg protein)	Enantio-selectivity (%ee, pro S)	Initial oxidation rate (nmol/min/mg protein)	Enantio-selectivity (%ee, pro S)
		o-Tyr (%)	m-Tyr (%)	p-Tyr (%)				
TOM	0.045	64	36	–	0.50	11	0.13	−4
ToMO	0.051	–	99	1	NA	NA	0.10	78
T4MO	0.023	–	63	37	0.07	−41	0.21	23
TpMO	0.064	–	64	36	NA	NA	0.03	62

NA—not active.

[a] Results for TOM and ToMO are based on 0.22 mg protein/ml/OD$_{600 nm}$ and for T4MO and TpMO on 0.24 mg protein/ml/OD$_{600 nm}$.

[b] Reported by Brouk and Fishman with initial substrate concentrations of 0.25 mM and standard deviation of less than 9% [25].

[c] Reported by Feingersch et al. with initial substrate concentrations of 1 mM and standard deviation of less than 10% [26].

[d] The initial styrene oxidation rates are based on GC/MS analysis with initial substrate concentrations of 1 mM. Enantio-selectivity (%ee) was determined after 2 h by analyzing the samples by GC/FID equipped with a chiral column. Results represent an average of at least two independent experiments with the absolute measured error being less than 10%.

Whole-cell biotransformations of the variants obtained from the screen (Fig. 3) revealed that replacing the polar Asp residue at position 285 to the apolar residues Ala, Leu or Ile increased the enzyme activity by 2.7-, 5.4- and 6.6-fold, respectively. Interestingly, the PEA oxidation rate increased with the hydrophobicity of the amino acid side chain. Moreover, replacing the negatively charged Asp 285 with uncharged residues (at pH 7), as Tyr, Pro, Cys or Gln, resulted with increased activity of 3-, 3.3-, 4- and 10.5-fold, respectively. Variant D285S, which is the analogous residue in ToMO (and was not found in the screen), had an activity of 0.017 ± 0.002 nmol/min/mg protein which is only 70% of WT activity. Despite the increase in oxidation rate for the different D285 variants, there was no change in regioselectivity (Fig. 3B). Surprisingly, examining the activity of the improved D285 variants on m- and p-tyrosol (Fig. 2A) as substrates (data not shown)

Fig. 2. The different reactions used in this study. (A) Regioselective hydroxylation of PEA to form p-tyrosol or m-tyrosol which could be further oxidized to form hydroxytyrosol, (B) enantioselective sulfoxidation of methyl-p-tolyl sulfide to (S)- or (R)-methyl p-tolyl sulfoxide, (C) enantioselective epoxidation of styrene to (S)- or (R)-styrene oxide.

revealed that unlike WT T4MO, they were all capable of oxidizing the tyrosol isomers to form hydroxytyrosol, but at very low conversion rates (with the exception of D285P). Likewise, employing o-tyrosol as a substrate resulted in the formation of two substituted dihydroxy benzenes, namely, 2,3-dihydroxyphenyl ethanol and 2,5-dihydroxyphenyl ethanol. These results demonstrate the ability of T4MO variants to form hydroxytyrosol, and emphasize the difficulty of polar and bulky substances to enter the tunnel and reach the active site.
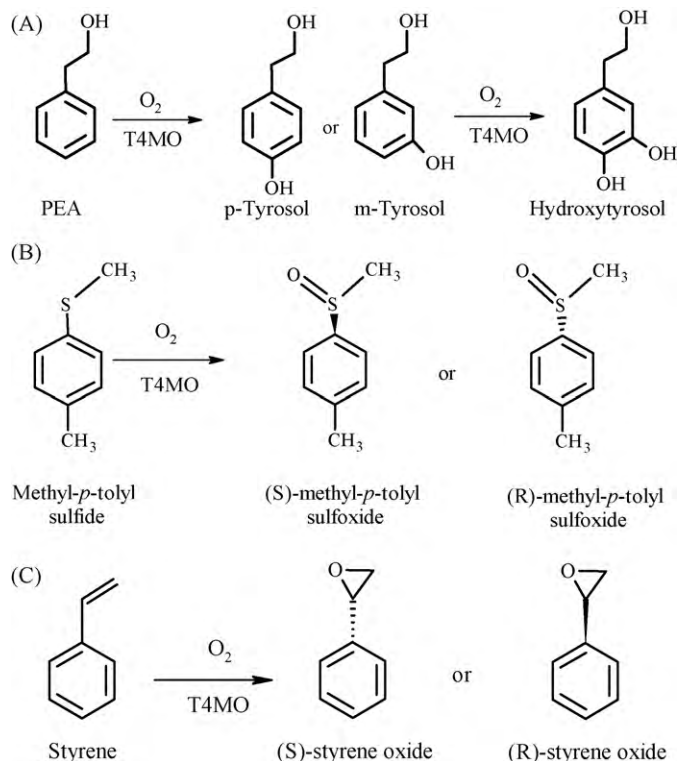
Similarly to our results, position TouA E214 in ToMO, located in the tunnel entrance, facing residue 285, was found by Vardar et al. [9] to influence rate but not regioselectivity of o- and p-nitrophenol hydroxylation. In was shown that the size of the residue at position 214 is most likely to be the factor influencing the oxidation rate, reaching up to 15-fold improvement for p-nitrophenol oxidation by ToMO E214G. The regioselectivity of all E214 variants tested remained the same.

From the results presented in Fig. 3 and the low activity of D285S it can be concluded that the acidic character of Asp 285 in the tunnel entrance has a higher impact than its size, on the enzyme activity toward PEA. As expected, changing the entrance of the tunnel did not affect the regioselectivity of the enzyme. The ability of the improved D285 variants to oxidize tyrosol isomers provides further evidence for the impact of the polar acidic residue of Asp 285 on the entrance of polar substrates through the tunnel.

3.3. Sulfoxidation of methyl-p-tolyl sulfide by WT and D285 variants

Chiral sulfoxides have been in focus of attention in recent years, especially in the chemical and pharmaceutical industries [35,36]. In recent work performed in our lab, TMOs were evaluated for their sulfoxidation activity using two model substrates, thioanisole and methyl-p-tolyl sulfide [26]. Although all four WT TMOs were able to oxidize thioanisole, only TOM and T4MO were active on methyl-p-tolyl sulfide (Table 2). It was shown that the presence of a side residue on the aromatic ring (as in methyl-p-tolyl sulfide) reduces dramatically the activity and the selectivity of TMOs [26]. For instance, the oxidation rate of methyl-p-tolyl sulfide by WT T4MO was one order of magnitude lower than the one on thioanisole, which is 1 Å shorter. Therefore, in the purpose of improving the enzyme activity towards enlarged substrates, the T4MO D285 library was screened on methyl-p-tolyl sulfide.
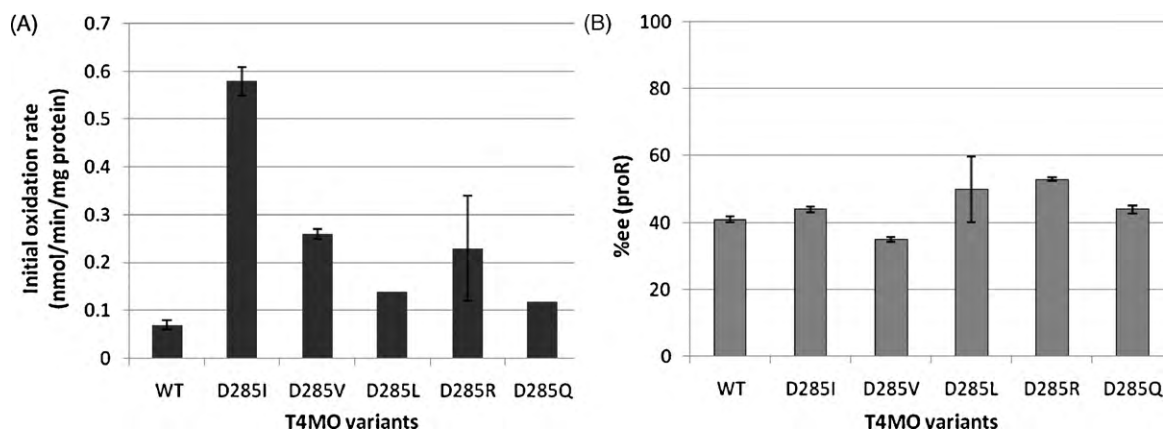
The most active variants were sequenced to give a total of 5 different mutations: D285I, D285V, D285L, D285R and D285Q. The best performing variant obtained following whole-cell biotransformation was D285I (Fig. 4). It had an 8-fold improvement in oxidation rate. Substitution of the polar and acidic residue Asp, to the apolar and aliphatic residues Val and Leu lead to increased enzy-
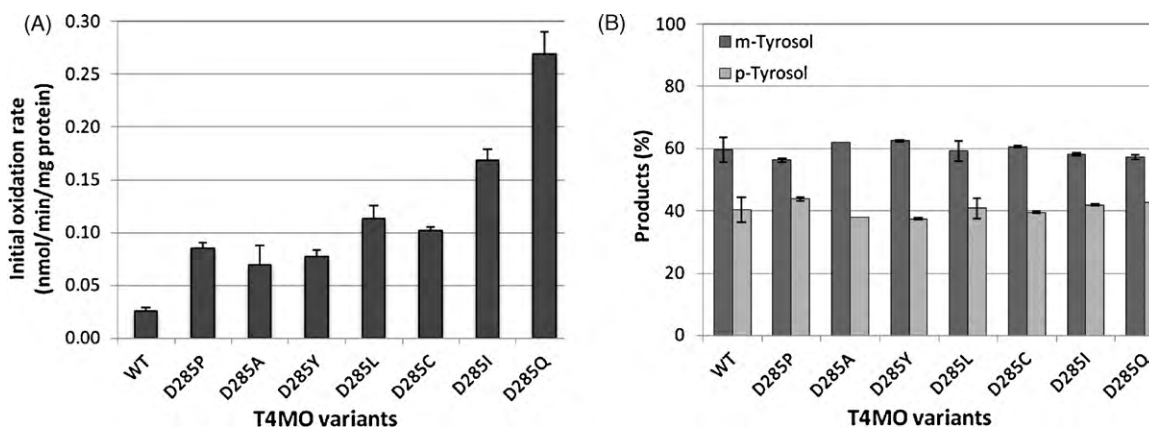
Fig. 3. Initial oxidation rate of PEA (A) by T4MO D285 variants and the product distribution (B). The activity was determined via HPLC analysis over a 2-h time period and regiospecificity was determined via GC/MS analysis after 24 h, with initial PEA concentration of 0.25 mM.

Fig. 4. Initial oxidation rate of methyl-*p*-tolyl sulfide (A) by T4MO D285 variants and the enantiomeric excess (proR) (B). The activity and the enantio-selectivity were determined via GC analysis over 2 and 24 h time period, respectively with initial substrate concentration of 1 mM.

matic activity of 3.7- and 2-fold, respectively. Moreover, replacing the acidic Asp with a polar but basic residue Arg, or uncharged (at pH 7) as Gln, resulted in increased activity of 3.2- and 1.7-fold, respectively. It should be noted that both the orientation and the size of the changed residue should be taken into consideration. As hypothesized, the alteration at position D285 lead to increased activity, but did not change the enantio-selectivity of the variants (Fig. 4B).

3.4. Epoxidation of styrene by WT and the D285 variants

Chiral epoxides are important intermediates in the chemical synthesis of optically active pharmaceuticals, polymers and agrochemicals. Enantiopure styrene oxide, an epoxide derived from styrene, may be used to synthesize enantiopure pharmaceuticals such as anti-diabetic agents and dopamine agonists [37]. To date only a single publication dealing with epoxidation reactions by TMOs has been published. In their article, McClay et al. [38] reported the oxidation of short-chain alkenes to their corresponding epoxides by several toluene monooxygenases, but styrene was not included in that work. However, other monooxygenases such as styrene monooxygenase, cytochrome P450 and *p*-cymene monooxygenase have been reported to oxidize styrene selectively [39–41].

Initially, four WT TMOs were evaluated for their ability to oxidize styrene to styrene-oxide (Fig. 2). The results clearly indicated that T4MO has the highest activity rate of 0.21 nmol/min/mg protein with low enantio-selectivity of 23% ee (pro S) (Table 2).

For further improvement of the T4MO activity, the randomized T4MO TmoA D285 library was screened using the pNTP assay which is based on the discoloration of pNTP in reaction with styrene oxide [32,33]. Using this screening method, 352 T4MO D285 variants were screened and those that showed an absorbance of 0.3 U below the WT enzyme were screened again in a one-point-biotransformation procedure using GC analysis. The most active variant had a smaller and slightly charged residue, Ser, at position 285. T4MO D285S had an improved epoxidation rate of 0.36 nmol/min/mg protein which is 1.7-fold higher than WT T4MO. As was expected, the enantio-selectivity of D285S was similar to that of WT (25% ee, pro S).

3.5. The effect of mutating the active site vs. the tunnel entrance

As hypothesized and demonstrated by the results, mutating a residue located in the entrance of the tunnel leading to the active site, enhanced the oxidation rate of all three substrates but had no effect on the regio- or enantio-selectivity. We further investigated this in comparison with mutations in the vicinity of the active site.

Recently, the influence of position I100 in T4MO on PEA oxidation rate and regioselectivity was published [25]. This residue (Fig. 1) was proposed to act as a gate to the diiron active site pocket [15,17,18,26]. It was discovered that increasing the size of the active site pocket and enlarging its entrance, by generating mutations at position I100, improves the oxidation rate and regioselectivity. Furthermore, it enabled hydroxytyrosol formation, which WT T4MO was not capable of producing [25]. Consequently, here we

Table 3
Relative activity and selectivity of T4MO variants mutated in the entrance to the tunnel and/or the active site.

| Activity tested	Substrate	T4MO variant	Mutation site	Relative activity[a]	Product distribution			Enantio-selectivity (pro S) (%)
					o-Tyr (%)	*m*-Tyr (%)	*p*-Tyr (%)	
Hydroxylation	PEA	WT	–	1	–	63	37	
		D285Q	Tunnel	11.7	–	57	43	
		D285I	Tunnel	7.4	–	58	42	
		I100A	Active site	35	–	92	8	
		I100A/D285Q	Both	85	–	91	9	
		I100A/D285I	Both	52	–	93	7	
Sulfoxidation	Methyl-*p*-tolyl sulfide	WT	–	1				−41
		D285I	Tunnel	8.3				−44
		I100A	Active site	8.6				79
		I100G	Active site	11.0				77
		I100A/D285I	Both	12.6				80
		I100G/D285I	Both	14.1				82
Epoxidation	Styrene	WT	–	1				23
		D285S	Tunnel	1.7				25
		I100L	Active site	0.9				58
		I100L/D285S	Both	1.4				52

[a] Relative activity is calculated as the initial oxidation rate normalized to WT T4MO. WT is designated as 1 with an activity of 0.023 ± 0.001, 0.07 ± 0.01 and 0.21 ± 0.02 nmol/min/mg protein for PEA, methyl-*p*-tolyl sulfide and styrene oxidation, respectivly. Reaction conditions were as described in the legend of Table 2. Results represent an average of at least two independent experiments with the absolute measured error being less than 10%.

examined the effect of combining efficient mutations at the tunnel and the active site. Using site-directed mutagenesis, the D285Q and D285I substitutions were introduced into the plasmid of I100A variant, which had the highest activity towards PEA among all the I100 variants tested. While variant D285Q had improved activity of 11.7-fold with similar regioselectivity as WT, and variant I100A had improved oxidation rate of 35-fold and preferred regioselectivity towards the *meta* position (92%), the double mutant I100A/D285Q showed improved activity of 85-fold and a regioselectivity similar to the I100A variant (Table 3). The same tendency was observed for the I100A/D285I variant which had improved activity of 52-fold and a regioselectivity of 93% towards the *meta* position. It can be concluded that combining mutations in the active site and in the tunnel entrance resulted in a synergistic effect on PEA oxidation rate, while the regioselectivity was influenced only by the active site mutation.

The importance of position I100 in T4MO was also reported for sulfoxidation [26]. The activity towards methyl-*p*-tolyl sulfide was improved significantly by all the I100 variants tested. While WT T4MO had a very low transformation rate with pro-R enantio-selectivity, all the I100 mutants changed their enantio preference to the S configuration [26]. The most improved variants, I100A and I100G, oxidized methyl-*p*-tolyl sulfide 8.6- and 11-fold faster than WT with enantio-selectivity of 79% and 77% pro-S, respectively (Table 3). D285I, the most active mutant found from the D285 library, had improved activity of 8.3-fold and enantio-selectivity similar to WT (44% pro-R). Generating double mutants in positions I100 and D285 resulted in both higher sulfoxidation rate and high pro-S enantio-selectivity (Table 3). Variant I100A/D285I had improved activity of 12.6-fold with enantio-selectivity of 80% pro-S. Likewise, variant I100G/D285I had improved activity of 14.1-fold with enantio-selectivity of 82% pro-S.

Position I100 was also tested for its influence on epoxidation activity. A library of T4MO TmoA I100 variants [26] was screened for improved activity towards styrene. The most active mutant was found to be T4MO I100L. Further investigation of the mutant activity showed a similar reaction rate as WT, but with improved enantio-selectivity of 58% pro-S *vs.* 25% for WT (Table 3). The substitution of Asp to Ser at position 285 in the T4MO I100L plasmid, by site-directed mutagenesis, resulted in increased activity and enantioselectivity of the double mutant. A 1.4-fold improvement in the epoxidation activity of variant I100L/D285S was gained by the D285S mutation while enantioselectivity of 52% pro-S was gained from the I100L substitution (Table 3).
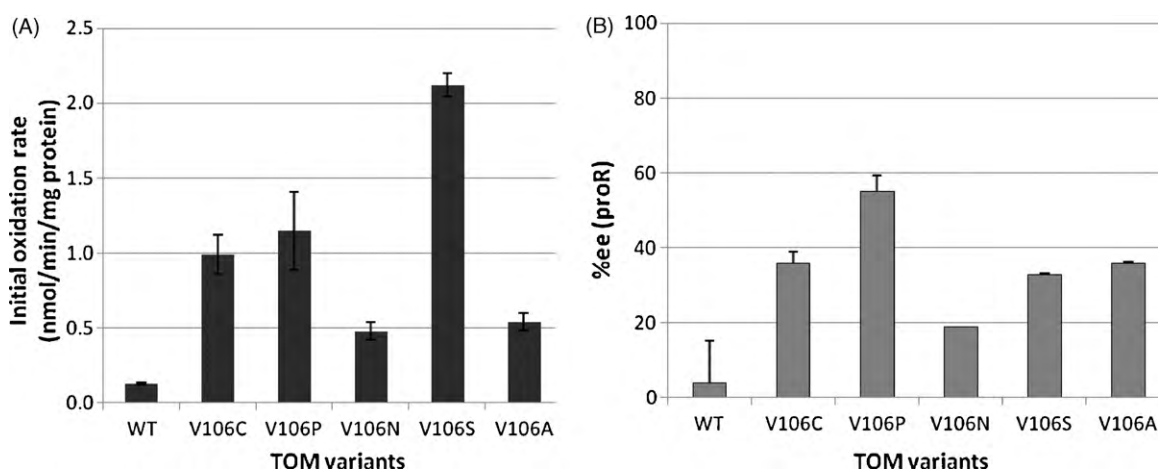
Fig. 5. Initial epoxidation rate of styrene (A) and enantio-selectivity towards the R-enantiomer (B) by WT TOM and TomA3 V106 mutants. Initial substrate concentration was 1 mM styrene.

Table 4
Relative activity on toluene, PEA, methyl-p-tolyl sulfide and styrene, by TG1 cells expressing T4MO variants.

| Initial substrate concentration | Relative activity on different substrates | | | | |
| | 0.25 mM | | 1 mM | | |
T4MO variant	Toluene[b]	PEA[a]	Toluene[b]	Methyl-p-tolyl sulfide[a]	Styrene[a]
WT	1	1	1	1	1
D285Q	4.6	11.7	1.6	1.7	NE
D285S	NE	0.7	5.8	NE	1.7
I100A/D285Q	5.4	85	NE	NE	NE

NE, not examined.

[a] Relative activity is calculated as the initial oxidation rate normalized to WT T4MO. WT is designated as 1 with an activity of 0.023 ± 0.001, 0.07 ± 0.01 and 0.21 ± 0.02 nmol/min/mg protein for PEA, methyl-p-tolyl sulfide and styrene oxidation, respectivly. Reaction conditions were as described in the legend of Table 2.

[b] Relative activity is calculated as the initial oxidation rate normalized to WT T4MO. WT is designated as 1 with an activity of 1.67 ± 0.01 and 6.6 ± 0.6 nmol/min/mg protein for initial toluene concentrations of 0.25 mM and 1 mM, respectivly, based on a Henry's law constant of 0.27 (0.89 mM and 3.56 mM, respectively, added if all the toluene in the liquid phase). Results represent an average of at least two independent experiments with the absolute measured error being less than 10%.

Residue TomA3 V106 in TOM, the analogous position of T4MO TmoA I100, was shown to have a major influence on rate and specificity [6]. Previously, we reported the effect of mutations at position TOM TomA3 V106 on the enzyme activity towards both PEA and methyl-p-tolyl sulfide [25,26]. It was found that mutations at position V106 can improve the PEA hydroxylation rate, compared to WT TOM, up to 39-fold (for V106E variant), and alter the regiospecificity of the enzyme dramatically [25]. Likewise, mutating position V106 affected the sulfoxidation activity and enantio-selectivity towards methyl-p-tolyl sulfide as a substrate [26]. Screening the TOM TomA3 V106 library for improved epoxidation activity towards styrene, resulted in five improved variants: V106C, V106P, V106N, V106S and V106A. Changing the Val residue at position 106, which is part of the hydrophobic cavity surrounding the diiron active site, affected both activity and enantio-selectivity of styrene epoxidation (Fig. 5). While WT TOM oxidized styrene with a rate of 0.13 nmol/min/mg protein and low enantio-selectivity of only 4% pro-R; a 17-fold improvement in rate was observed for V106S variant (33% ee, pro-R) and 14-fold improvement in enantio-selectivity was observed for the V106P variant (9-fold improvement in epoxidation rate). Additionally, mutants V106N, V106A and V106C displayed improved activity of 3.7-, 4.1- and 7.6-fold compared to WT TOM with pro-R enantios-electivity of 19%, 36% and 36%, respectively. These results further support the major influence that a residue in the entrance to the active site pocket has on enzyme activity and selectivity.

Altering residues situated in the entrance to the active site pocket, were previously reported to influence the oxidation rate of the natural substrate toluene. Fishman et al. reported an initial toluene oxidation rate of 4.4 nmol/min/mg protein by WT T4MO (with toluene concentration of 0.09 mM) while a 1.6- and 1.5-fold improvement was measured for variants I100A and I100S, respectively [18]. Likewise, Rui et al. reported an increased activity on toluene of different TOM V106 variants with up to 2.1-fold improvement by V106A (with toluene concentration of 0.09 mM) [31]. In the present work, we further examined the effect of amino acid substitutions in the tunnel entrance, in addition to the active site entrance, on toluene oxidation. The initial oxidation rate by WT T4MO was 1.67 and 6.6 nmol/min/mg protein for 0.25 mM and 1 mM toluene, respectively (Table 4). Expectedly, the toluene oxidation rates were 1–2 orders of magnitude higher than those of the unnatural substrates, PEA, methyl-p-tolyl sulfide and styrene. It was found that D285Q, which oxidized PEA (0.25 mM) 11.7-fold faster than WT, had an improved activity of 4.6-fold on toluene as well, with an initial oxidation rate of 7.7 nmol/min/mg protein. The initial oxidation rate of 1 mM toluene by variant D285Q was 1.6-fold higher than WT similarly to the improvement in oxidation of 1 mM methyl-p-tolyl sulfide. Combining the beneficial mutations, D285Q and I100A, which led to 85-fold improvement in the oxidation of 0.25 mM PEA, resulted with only 5.4-fold improvement

in toluene oxidation. Thus, the mutations were more valuable for increasing the rate of the larger substrate, PEA. The most significant improvement in activity on toluene was obtained by variant D285S, which exhibited a 1.7-fold improvement in the oxidation of 1 mM styrene. D285S oxidized toluene 5.8-fold faster than WT, reaching an initial oxidation rate of 38.4 nmol/min/mg protein. In sum, all of the variants examined showed an increase in toluene oxidation although they were screened for different substrates.

In the present work, in order to perform saturation mutagenesis at position T4MO TmoA D285, the conventional degenerate primers, consisting NNN codons, were used (N: adenine/cytosine/guanine/thymine). Recently, Reetz et al. introduced the use of NDT codon degeneracy (D: adenine/guanine/thymine; T: thymine) for constructing smaller libraries [42]. This option involves 12 codons and reduces the number of amino acid replacements to 12 (Phe, Leu, Ile, Val, Tyr, His, Asn, Asp, Cys, Arg, Ser, Gly). Although the NDT codon degeneracy requires the screening of only 34 clones in the case of one residue site [42], screening of T4MO TmoA D285 NDT-library would have hypotheticaly resulted with the finding of D285Y, D285L, D285C, D285I, D285V, D285S and D285R substitutions, but would have missed the D285Q, D285P and D285A substitutions, that were found to be beneficial. Likewise, constructing the T4MO TmoA I100 and TOM TomA3 V106 libraries using NDT primers would have led to the absence of T4MO I100A and TOM V106A variants that are reported here for their improved activity. Indeed, NDT codon degeneracy ensures a balanced mix of amino acids in terms of structural and electrostatic characteristics, but still, similar amino acids affect differently enzyme activity. For instance, structurally similar amino acids as Cys and Ser had an opposite effect on PEA oxidation when situated at position 285. While the D285C improved the PEA oxidation rate by 4-fold, the D285S substitution resulted with decreased activity on PEA. Similarly, substituting Asp to Ile resulted with an 8-fold improvement for methyl-p-tolyl sulfide oxidation rate, while substituting to the structurally similar Leu improved the enzyme activity by only 2-fold. Similar amino acids may also have a different affect on the enantio-selectivity of the enzyme, as in the case of T4MO I100L. A substitution of Ile with Leu improved the enantio-selectivity from 25% to 58% ee.

4. Conclusions

The results presented in this study, have shed some light on the role played by a key residue in the tunnel entrance, compared with the active site pocket entrance. The amino acid residue (D285) located at the entrance of the tunnel leading to the diiron center was mutated with the intention of accelerating the substrate/product flow to/from the active site. The effect of this modification on the catalytic properties of T4MO was determined by screening for three different activities: (1) hydroxylation of an aromatic substrate sub-

stituted with a polar and bulky residue (PEA), (2) sulfoxidation on the side chain of methyl-*p*-tolyl sulfide and (3) epoxidation on the double bond side chain of styrene (Fig. 2). Due to the distant location of D285 from the active site itself, it was hypothesized and demonstrated that alterations at this position affect the activity, but not the regio- or enantio-selectivity. In contrast, mutating a residue that is part of the hydrophobic gate in the active site entrance, i.e. position T4MO I100 and TOM V106, affected both activity and selectivity. Mutating the entrance of the active site may have two implications. First, enlarging the hydrophobic gate allows easier access to/from the active site, which results in higher oxidation rates. Second, expanding the hydrophobic cavity surrounding the diiron binding site enables better or different alignment of the substrate in the active site thus influencing the regio- or enantio-selectivity. Combining the effects by mutating both "gates", to the active site along with the tunnel entrance, results in obtaining an additive or even synergistic outcome on the enzyme activity.

With the intention of rationally designing an enzyme, it is important to consider, not only the enzyme structure and function, but also the substrate characteristics. WT T4MO oxidized the natural substrate, toluene, having a small and hydrophobic side chain, 1–2 orders of magnitude faster than other structurally related substrates, as PEA, methyl-*p*-tolyl sulfide and styrene. Besides toluene, the fastest oxidation rate was obtained for 1 mM styrene (0.21 nmol/min/mg protein), which has a relatively small and rigid allylic side chain, while the oxidation rate of 1 mM PEA, with the polar and bulky side chain, was the slowest with a rate of 0.06 nmol/min/mg protein. For the improvement of activity towards PEA, the removal of the negative electrostatic charge in the tunnel entrance was more important, whereas for styrene, a higher impact was achieved by enlarging the width of the tunnel entrance. In addition to the size of the amino acid side chain, it is important to consider its rotamer configuration. Generally, the improvement obtained by mutating the tunnel entrance was lower for styrene oxidation compared with PEA and methyl-*p*-tolyl sulfide (Table 3). Similarly, altering the active site entrance affected mostly the enzyme activity toward PEA, with improvement of up to 35-fold by T4MO I100A, compared with improvement of up to 11-fold for methyl-*p*-tolyl sulfide oxidation (by T4MO I100G) and no activation for styrene (by T4MO I100L). Interestingly, while different substitutions, as D285I and D285Q, were beneficial for the oxidation of both PEA and methyl-*p*-tolyl sulfide, they affected negatively the enzyme activity towards styrene. Likewise, substitution D285S, which improved the styrene oxidation rate, had a negative effect on the enzyme activity towards PEA. The results demonstrate that altering a key residue can be beneficial for improving the enzyme's activity towards diverse substrates, but the extent of the improvement is different for each one.

In summary, the amino acid replacement at "hot spots" is substrate dependant. In addition, the location of the key residue in the protein architecture will determine the nature of the change in activity. Mutations at the tunnel entrance will most likely affect the activity rate whereas altering residues near the active site can affect both rate and selectivity.

Acknowledgment

References

[1] A. Schmid, J.S. Dordick, B. Hauer, A. Kiener, M. Wubbolts, B. Witholt, Nature 409 (2001) 258–268.
[2] T.W. Johannes, H. Zhao, Curr. Opin. Microbiol. 9 (2006) 261–267.
[3] M. Leisola, O. Turunen, Appl. Microbiol. Biotechnol. 75 (2007) 1225–1232.
[4] N.M. Antikainen, S.F. Martin, Bioorg. Med. Chem. 13 (2005) 2701–2716.
[5] K.L. Morley, R.J. Kazlauskas, Trends Biotechnol. 23 (2005) 231–237.
[6] A. Fishman, Y. Tao, G. Vardar, L. Rui, T.K. Wood, in: J.-L. Ramos, R.C. Levesque (Eds.), Pseudomonas, Springer, US, 2006, pp. 237–286.
[7] J. Sylvestre, H. Chautard, F. Cedrone, M. Delcourt, Org. Process Res. Dev. 10 (2006) 562–571.
[8] S.B. Rubin-Pitel, H. Zhao, Comb.Chem. High Throughput Screen. 9 (2006) 247–257.
[9] G. Vardar, T.K. Wood, J. Bacteriol. 187 (2005) 1511–1514.
[10] G. Vardar, K. Ryu, T.K. Wood, J. Biotechnol. 115 (2005) 145–156.
[11] J. Schmitt, S. Brocca, R.D. Schmid, J. Pleiss, Protein Eng. 15 (2002) 595–601.
[12] I. Capila, Y. Wu, D.W. Rethwisch, A. Matte, M. Cygler, R.J. Linhardt, Biochim. Biophys. Acta 1597 (2002) 260–270.
[13] R. Chaloupkova, J. Sykorova, Z. Prokop, A. Jesenska, M. Monincova, M. Pavlova, M. Tsuda, Y. Nagata, J. Damborsky, J. Biol. Chem. 278 (2003) 52622–52628.
[14] M. Pavlova, M. Klvana, Z. Prokop, R. Chaloupkova, P. Banas, M. Otyepka, R.C. Wade, M. Tsuda, Y. Nagata, J. Damborsky, Nat. Chem. Biol. 5 (2009) 727–733.
[15] K.A. Canada, S. Iwashita, H. Shim, T.K. Wood, J. Bacteriol. 184 (2002) 344–349.
[16] G. Vardar, T.K. Wood, Appl. Environ. Microbiol. 70 (2004) 3253–3262.
[17] Y. Tao, A. Fishman, W.E. Bentley, T.K. Wood, J. Bacteriol. 186 (2004) 4705–4713.
[18] A. Fishman, Y. Tao, W.E. Bentley, T.K. Wood, Biotechnol. Bioeng. 87 (2004) 779–790.
[19] L.J. Bailey, J.G. McCoy, G.N. Phillips, B.G. Fox, Proc. Natl. Acad. Sci. U.S.A. 105 (2008) 19194–19198.
[20] J.G. Leahy, P.J. Batchelor, S.M. Morcomb, FEMS Microbiol. Rev. 27 (2003) 449–479.
[21] K.H. Mitchell, J.M. Studts, B.G. Fox, Biochemistry 41 (2002) 3176–3188.
[22] J. Sambbrook, D.W. Russell, Molecular Cloning: A Laboratory Manual, third ed., Cold Spring Harbor Laboratory Press, New York, 2001.
[23] Y. Tao, A. Fishman, W.E. Bentley, T.K. Wood, Appl. Environ. Microbiol. 70 (2004) 3814–3820.
[24] G. Vardar, T.K. Wood, Appl. Microbiol. Biotechnol. 68 (2005) 510–517.
[25] M. Brouk, A. Fishman, Food Chem. 116 (2009) 114–121.
[26] R. Feingersch, J. Shainsky, T.K. Wood, A. Fishman, Appl. Environ. Microbiol. 74 (2008) 1555–1566.
[27] R.W. Eaton, P.J. Chapman, J. Bacteriol. 177 (1995) 6983–6988.
[28] L. Rui, K.F. Reardon, T.K. Wood, Appl. Microbiol. Biotechnol. 66 (2005) 422–429.
[29] A. Fishman, Y. Tao, L. Rui, T.K. Wood, J. Biol. Chem. 280 (2005) 506–514.
[30] J. Dolfing, A.J. van den Wijngaard, D.B. Janssen, Biodegradation 4 (1993) 261–282.
[31] L. Rui, Y.M. Kwon, A. Fishman, K.F. Reardon, T.K. Wood, Appl. Environ. Microbiol. 70 (2004) 3246–3252.
[32] K. Tee, O. Dmytrenko, K. Otto, A. Schmid, U. Schwaneberg, J. Mol. Catal. B: Enzyme 50 (2008) 121–127.
[33] K. Tee, U. Schwaneberg, Comb. Chem. High Throughput Screen. 10 (2007) 197–217.
[34] M.H. Sazinsky, J. Bard, A. Di Donato, S.J. Lippard, J. Biol. Chem. 279 (2004) 30600–30610.
[35] R. Patel, Coord. Chem. Rev. 252 (2008) 659–701.
[36] R. Bentley, Chem. Soc. Rev. 34 (2005) 609–624.
[37] A. Archelas, R. Furstoss, Annu. Rev. Microbiol. 51 (1997) 491–525.
[38] K. McClay, B. Fox, R. Steffan, Appl. Environ. Microbiol. 66 (2000) 1877–1882.
[39] S. Panke, M. Held, M.G. Wubbolts, B. Witholt, A. Schmid, Biotechnol. Bioeng. 80 (2002) 33–41.
[40] E. Farinas, M. Alcalde, F. Arnold, Tetrahedron 60 (2004) 525–528.
[41] T. Nishio, A. Patel, Y. Wang, P.C. Lau, Appl. Microbiol. Biotechnol. 55 (2001) 321–325.
[42] M.T. Reetz, D. Kahakeaw, R. Lohmer, Chembiochem 9 (2008) 1797–1804.